J. Membrane Biol. 142, 363–379 (1994)

The Journal of
Membrane
Biology

Properties of the K^+ Inward Rectifier in the Plasma Membrane of Xylem Parenchyma Cells from Barley Roots: Effects of TEA^+, Ca^{2+}, Ba^{2+} and La^{3+}

L.H. Wegner[1], A.H. De Boer[1], K. Raschke[2]

[1]Vrije Universiteit Amsterdam, Department of Plant Physiology and Biochemistry, Institute of Molecular Biological Sciences, BioCentrum Amsterdam, De Boelelaan 1087, NL-1081 HV Amsterdam, The Netherlands

[2]Pflanzenphysiologisches Institut und Botanischer Garten, Untere Karspüle 2, D 37073 Göttingen, Germany

Received: 23 May 1994/Revised: 1 September 1994

Abstract. Xylem parenchyma cells are situated around the (apoplastic) xylem vessels and are involved in the control of the composition of the xylem sap by exporting and resorbing solutes. We investigated properties of the K^+ inward rectifier in the plasma membrane of these cells by performing patch clamp experiments on protoplasts in the whole-cell configuration. Inward currents were sensitive to the K^+ channel blocker TEA^+ at a high concentration (20 mM). Barium, another "classical" K^+ channel blocker, inhibited K^+ currents with a K_i of about 1.3 mM. In contrast to guard cells, the cytosolic Ca^{2+} level proved to be ineffective in regulating the K^+ conductance at hyperpolarization. External Ca^{2+} blocked currents weakly in a voltage-dependent manner. From instantaneous current-voltage curves, we identified a binding site in the channel pore with an electrical distance of about 0.2 to 0.5. Lanthanum ions reduced the inward current in a voltage-dependent manner and simultaneously displaced the voltage at which half of the channels are in the open state to more positive values. This finding was interpreted as resulting from a sum of two molecular effects, an interaction with the mouth of the channel that causes a reduction of current, and a binding to the voltage sensor, leading to a shielding of surface charges and, subsequently, a modulation of channel gating.

A comparison between the K^+ inward rectifier in xylem parenchyma cells, guard cells and KAT1 from *Arabidopsis* leads to the conclusion that these rectifiers form subtypes within one class of ion channels. The ineffectiveness of Ca^{2+} to control K^+ influx in xylem parenchyma cells is interpreted in physiological terms.

Correspondence to: A.H. De Boer

Key words: Root — Xylem parenchyma cell — K^+ inward rectifier — Ca^{2+} — La^{3+} — Ba^{2+}

Introduction

Xylem parenchyma cells in roots form the inner boundary of the symplastic continuum that extends from the cortex into the stele, where long distance transport to the shoot occurs via the xylem vessels. Radial movement of salts from the soil solution to the xylem sap is predominantly symplastic and, hence, includes a release across the plasma membrane of the xylem parenchyma cells as the final step. In a previous study (Wegner & Raschke, 1994), we characterized two types of outward rectifiers selective for cations as well as an anion channel that could serve as a pathway for salt release. Xylem parenchyma cells also have the capacity to resorb ions, a function that prevails in "ion consuming" parts of the plant like growing stems. The uptake of K^+ from the xylem sap has been postulated to occur by a "chemiosmotic" mechanism (De Boer et al., 1985): A hyperpolarization of the plasma membrane by H^+ ATPase activity provides the driving force for a "passive" K^+ influx into the xylem parenchyma cell (The concentration gradient for K^+ between symplast and xylem sap depends on the physiological situation (Clarkson, 1993), but is persistently uphill for K^+ uptake by the cell.). In the previous study (Wegner & Raschke, 1994), we reported on a K^+-selective inwardly rectifying conductance (KIRC), active at voltages more negative than about −110 mV, which presumably serves the function of K^+ resorption from the xylem sap. The rectifier was shown to translocate K^+, and, to a lesser extent, also Rb^+, Cs^+, Li^+ and Na^+, but not anions.

Inwardly rectifying conductances selective for K^+

have also been found in the plasma membrane of various other plant cells, including guard cells and mesophyll cells, from several species (Hedrich & Schroeder, 1989, Tester, 1990). From electrophysiological measurements, it is not yet clear to what extent the properties of these K^+ conductances vary among different cell types. Recently, two genes (KAT1 and AKT1) with high homology, encoding for inwardly rectifying channels, have been identified in *Arabidopsis* (Anderson et al., 1992; Sentenac et al., 1992). One of the channels (KAT1) was expressed in oocytes and characterized with respect to its electrophysiological properties (Schachtman et al., 1992). Interestingly, AKT1 was predominantly expressed in roots (Basset et al., 1993), indicating that cell-specific variations of channels among different plant organs and cell types could have a genetic origin (Jan & Jan, 1990).

The rationale of our work was to provide an electrophysiological basis for a comparison of the inward rectifier in xylem parenchyma cells with channels of similar properties and physiological functions in other cell types, aiming at a better understanding of the complexity of ion channels in plant tissues. In the first place, we will compare our data to those obtained by others on guard cells, since this object has captured most attention by plant electrophysiologists recently, and since the K^+ inward rectifier has been characterized thoroughly in this cell type (Schroeder, Raschke & Neher, 1987; Schroeder, 1988; Blatt, 1992; Fairey-Grenot & Assmann, 1992*a,b*).

Moreover, the blocker studies that were done by us render information on the mechanism of ion translocation and on the channel structure (Tester, 1988*a,b*). Part of the data has been published elsewhere in preliminary form (Wegner & Raschke, 1992; Wegner, Raschke, & De Boer, 1993).

Materials and Methods

Plant Cultivation, Preparation of Protoplasts

Plant cultivation, the isolation procedure for xylem parenchyma protoplasts, and the electrical recordings were described in detail elsewhere (Wegner & Raschke, 1994). Briefly, "high salt" barley seedlings (*Hordeum vulgare* cv. Apex) were grown on hydroponics with a 6/18 hr dark/light cycle at 20 and 22°C, respectively. Plants were harvested after 3–5 weeks. Protoplasts were obtained from isolated steles of nodal roots 0.7–1.5 cm above the root tip by an enzymatic digestion with 2% w/v Onozuka R10, 0.02% w/v Pectolyase, 2% w/v BSA, 10 mM Na-ascorbate and 1 mM $CaCl_2$, π = 500 mOsmol/kg (mannitol), pH 5.5. The selectivity of the isolation procedure was based on the time sequence of protoplast release: The cells involved in xylem loading and unloading are those of the early metaxylem that forms a ring in the periphery of the stele, alternating with the phloem. Cell walls in this part of the stele remain unlignified (with the exception of the early metaxylem vessels themselves), in contrast to the center of the stele and most of the pericycle. Protoplasts from early metaxylem are released well ahead of those from other tissues in the stele, as lignification slows down cell wall digestion (We could show that no protoplasts came from the phloem (Wegner & Raschke, 1994)). After 2 hr of incubation, the suspension was poured on a 20 μm net, washed with 500 mM mannitol, 1 mM $CaCl_2$, centrifuged at 700 *g* and resuspended in about 100 μl wash medium.

Electrophysiology

Patch clamp experiments in the whole-cell configuration (Hamill et al., 1981) were performed using an EPC7 amplifier (List Electronics, Darmstadt, Germany). Data were low-pass filtered with an 8-pole Bessel filter (Frequency Devices, Haverhill, MA) at 500 Hz and digitized with an ITC16 interface (Instrutech, Elmont, NY) with a sample rate of 2 kHz. For generation of pulse protocols and storing and evaluating data, an Atari Mega ST 4 computer (Atari, Sunnyvale, CA) and software from Instrutech were used. Some of the experiments were done on a different setup, equipped with an Axopatch 200A amplifier (Axon Instruments, Foster City, CA). Data were digitized with a CED 1400AD/DA converter and analyzed with a personal computer (HP Vectra 386), using EPC patch and voltage software (Patch and Vclamp version 5.0 from Cambridge Electronic Design (CED), Cambridge, UK).

Liquid junction potentials were corrected for (Neher, 1992). The reference electrode was connected via a salt bridge; junction potentials at the tip of the salt bridge resulting from an exchange of the bath solution were also corrected for. Equilibrium potentials were calculated from ion activities according to Robinson and Stokes (1968).

Solutions

If not stated otherwise, solutions with standard compositions (*see below*) were used. Blockers were applied by bath perfusion. Solutions were frozen at −20°C and thawed immediately before experiments were performed. Pipette solutions were filtered through 0.22 μm filters. Standard bath medium: 30 mM KCl or −glutamate, 10 mM HEPES, 2 mM $MgCl_2$, π = 500 mOsmol/kg (mannitol). The pH was adjusted to 5.8 using MES. (For Ca^{2+} concentrations, *see* specifications below and in the figure legends.) Standard pipette medium: 120 mM KCl, 10 mM Tris, 2 mM ATP, Mg^{2+}_{free} = 2 mM ($MgCl_2$), π = 530 mOsmol/kg (mannitol). The pH was adjusted to a value of 7.2 by adding Tris. (For Ca^{2+} concentrations, *see* specifications below and in the figure legends. If not stated otherwise, the final free Ca^{2+} concentration was 1 μM.)

The Ca^{2+} concentration in the bath was usually 1 mM (exceptions are mentioned in the legends) with either Cl^- or gluconate as counterions. For higher concentrations, only Ca^{2+}-gluconate was used. In pipette solutions, Ca^{2+} concentrations were buffered with either 10 mM EGTA (150 nM and 1 μM Ca^{2+}, respectively) or HEEDTA (10 μM). Amounts of Ca^{2+} to be added in order to adjust the free Ca^{2+} concentration at the desired level were calculated using a commercially available computer program (Führ, Warchol & Gratzl, 1993). Blockers (Ba^{2+}, La^{3+}, TEA^+) were used as Cl^- salts.

Abbreviations

$E_{rev.}$, reversal potential; E_x, equilibrium potential of the ion species *x;* HEEDTA, *N*-hydroxylethyl-ethylenediamine-triacetic acid; π, osmotic pressure; TEA^+, tetraethylammonium

Results

Inward currents recorded in the whole-cell configuration were interpreted as ensemble currents resulting from

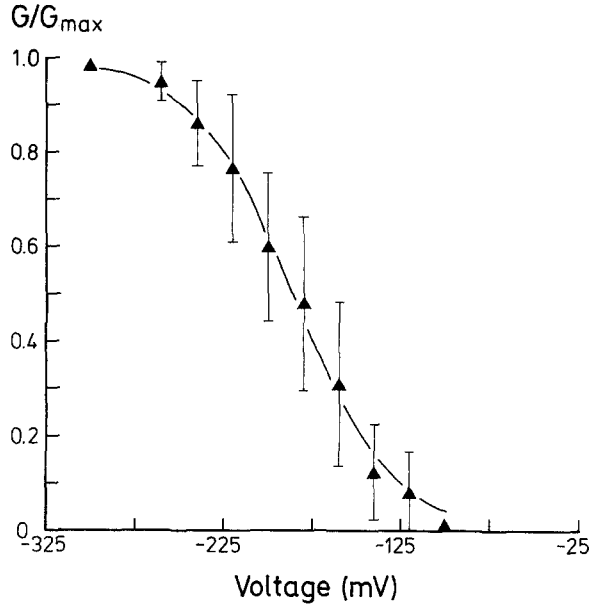

Fig. 1. The normalized chord conductance (G/G_{max}) of the K^+ inward rectifier plotted as a function of the membrane potential. Mean of 15 experiments (±SD). Data were fitted with a Boltzmann equation (Eq. 1) to specify gating characteristics (continuous line, for fit parameters, *see* Table 1).

multiple channel activity (*compare* traces of channel activation in Schroeder et al., 1987) and analyzed accordingly. Data analysis was based on the assumption that currents reflected the activity of one type of channel that dominated the conductance; no inconsistencies emerged from this approach. Figure 1 shows a plot of the relative chord conductance as a function of the clamped membrane potential. The voltage dependence of channel gating could be obtained by fitting these data with the following Boltzman term:

$$G/G_{max} = 1/(1 + \exp(\delta F(U_{1/2} - U)/RT)) \quad (1)$$

(Almers, 1978) with δ being the apparent, minimum gating charge, $U_{1/2}$ being the voltage of half-maximal conductance and U being the clamped voltage. The other variables have their usual meaning. The parameters of the optimal fit, corresponding to the continuous line in Fig. 1, are summarized in Table 1. In the previous publication (Wegner & Raschke, 1994), we showed that inward currents are carried by potassium ions (and thus form a pathway for K^+ uptake). To evaluate the substrate dependence of the inward rectifier in the millimolar range, we recorded inward K^+ currents at three different K^+ concentrations in the bath. The current-voltage plots in Fig. 2 clearly show that the "activation potential" did not shift with the equilibrium potential for K^+ and that the voltage dependence was almost identical at 10 and

Table 1. Gating properties of the inward rectifier in guard cells and xylem parenchyma cells

	δ (Minimal gating charge)	$U_{1/2}$ (half-maximal gating voltage in mV)
Xylem parenchyma cell	1.16 ± 0.22^a	-188 ± 20^a
Guard cell	1.35 ± 0.04	-188 ± 3

[a] Mean ± SD for 15 experiments. Gating properties of the inward rectifier at standard conditions with 1 mM Ca^{2+} in the bath. Data (*see* Fig. 1) were fitted with a Boltzmann term as specified in the text (Eq. 1). For comparison, data on the guard cell inward rectifier are shown, cited from Blatt (1992).

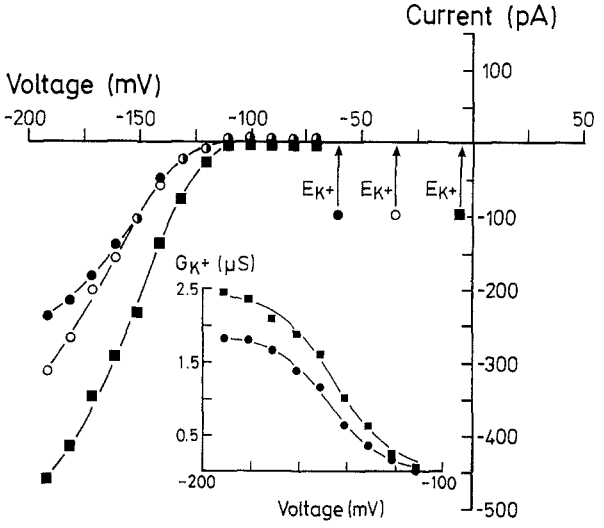

Fig. 2. Substrate dependence of the inward rectifier: Inward currents at (●) 10 mM; (○) 30 mM and (■) 100 mM K^+ in the bath. Current-voltage curves result from pulse protocols like the one shown in Fig. 3*A*, but the membrane was hyperpolarized from a holding potential of −60 mV in increments of 10 mV. Inset: Voltage dependence of the K^+ chord conductance at 10 and 100 mM K^+. The potentials of half-maximal conductance were −147 and −145 mV, respectively, indicating that gating was not affected by varying K^+ gradients across the membrane.

100 mM K^+ (*see inset*). Absolute chord conductances increased by about 25% upon increasing the K^+ concentration in the bath 10-fold.

We investigated the kinetics of the inward rectifier by fitting the time course of current activation and deactivation with exponential functions to current traces like those shown in Fig. 3*A*. Current activation was best described with a double-exponential function. The fast time constant decreased with hyperpolarization, ranging from about 120 msec at −120 mV to about 30 msec at −240 mV. The slow time constant, contributing less to the overall current amplitude, was in the range of 200–400 msec and voltage independent. In contrast, current deactivation was single exponential (data presented below to illustrate La^{3+} effects on the time constant).

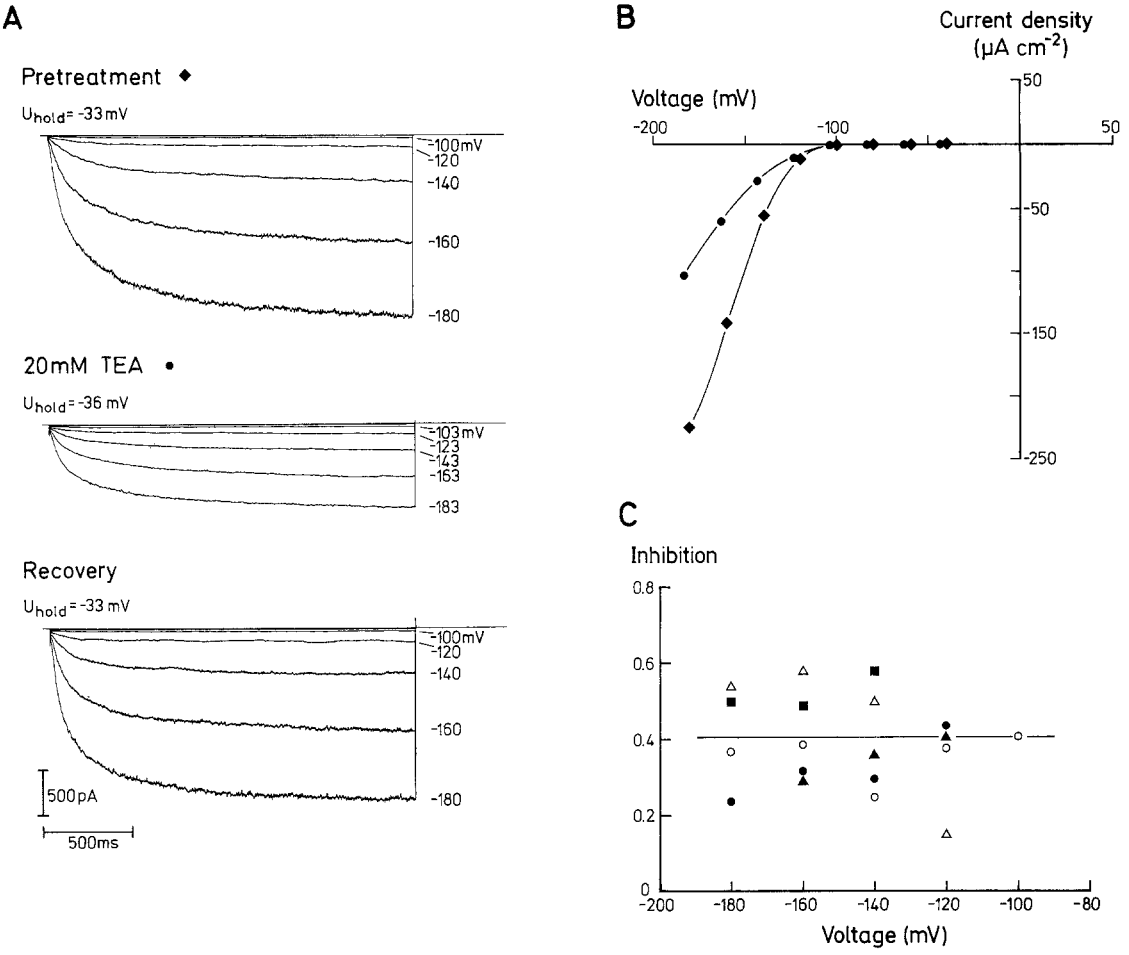

Fig. 3. Effects of TEA^+ on K^+ inward currents. (*A*) Superimposed current traces at pretreatment, after addition of 20 mM TEA^+ to the bath and after removal of TEA^+ (recovery). Pulse protocols as indicated in the figure close to current traces. Between individual 2 sec pulses, the membrane was clamped at the holding potential for 4 sec. Standard solutions were used, with 20 mM TEACl added for the treatment. (*B*) Current-voltage relations obtained from the experiment shown in *A*. Currents were normalized with respect to the membrane surface area of the protoplast. (♦) Pretreatment; (●) +20 mM TEA^+ (*C*) Fraction of current blocked by 20 mM TEA^+ for five protoplasts (different symbols) as a function of the clamped potential. Currents were reduced by about 40% in a voltage-independent manner as indicated by the horizontal line.

TEA^+

Inward K^+ currents were reduced by about 40% after exposing the plasma membrane to 20 mM TEACl in the bath (Fig. 3). The external K^+ concentration was kept at 30 mM. Steady-state currents were recorded by imposing negative-going voltage pulses in the whole-cell configuration prior to and after the addition of the blocker (Fig. 3*A,B*). Currents recovered fully after perfusion of the bath with TEA^+-free solution (*see* Fig. 3*A*). The effectiveness of the block varied somewhat among five individual cells (*see* data obtained from five protoplasts in Fig. 3*C*). Plotting the fraction of current inhibited by TEA^+ as a function of the clamped potential did not reveal a pronounced voltage dependence of the blockage (Fig. 3*C*).

Ca^{2+}

The activity of the K^+ inward rectifier in guard cells is strongly modulated by the cytosolic Ca^{2+} concentration (Schroeder & Hagiwara, 1989; Blatt, Thiel & Trentham 1991; Fairley-Grenot & Assmann 1992*a*). For xylem parenchyma cells, current-voltage curves recorded with 150 nM Ca^{2+} (corresponding to the presumed resting level of cytosolic Ca^{2+}, Schroeder & Thuleau, 1991) and 10 μM free Ca^{2+} in the pipette are shown in Fig. 4. Current densities were similar at 1 μM Ca^{2+} (*not shown*). Obviously, the K^+ inward rectifier in these cells does not respond to changes of the cytosolic Ca^{2+} level in the physiological range. The kinetic properties were not affected either (*not shown*). To facilitate the formation of "gigaseals" with 150 nM Ca^{2+} in the pipette, the very tip

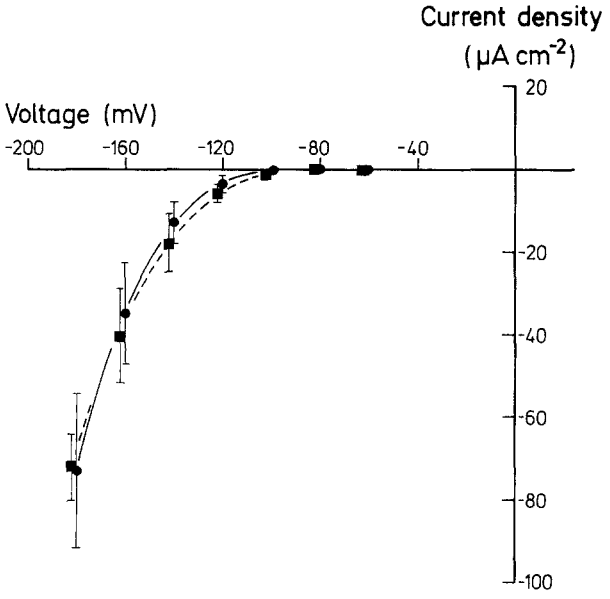

Fig. 4. Current-voltage curves (current densities) derived from whole-cell experiments with (●) 150 nM and (■) 10 μM free Ca^{2+} in the pipette solution. Mean values ± SDs obtained from four and eight protoplasts, respectively. The Ca^{2+} concentration in the bath was 1 mM. Pulse protocols were imposed as described in Fig. 3.

was filled with an unbuffered solution containing no Ca^{2+}, but of otherwise identical composition. To make sure that the presence of inward currents at "high Ca^{2+}" in the pipette was not due to poor control of cytosolic Ca^{2+}, a pulse protocol was imposed directly after seal formation (about 1 min) and repeated after 15 min. Current-voltage curves were almost identical (*not shown*), indicating that even after prolonged dialysis of the cytosol with an elevated Ca^{2+} concentration in the pipette, the magnitude of the inward currents was not reduced.

The effect of external Ca^{2+} on the inward rectifier was studied by perfusion of the bath with media differing in Ca^{2+} concentration. Identical voltage clamp protocols were imposed at each of these concentrations (Fig. 5). Short pulse times (usually 750 msec) were chosen, as prolonged hyperpolarization would cause a breakdown of the plasma membrane. If pulse times were not sufficiently long for a complete activation of whole-cell currents, the steady-state level was obtained by extrapolation of current traces to infinity. As shown by Fig. 5*B*, elevation of the external Ca^{2+} concentration about 1 mM (10 and 40 mM) resulted in a slight, voltage-dependent reduction of inward currents. The block by Ca^{2+} manifested itself at voltages below about −180 mV and increased with hyperpolarization. The effect was fully reversible.

Pulse protocols like this one were not suitable to distinguish between a voltage-dependent modulation of channel gating and a blockade of the pore due to Ca^{2+} binding (open channel blockade). Therefore, double-pulse protocols were imposed as shown in Fig. 6. Inward currents were activated by an identical prepulse and, subsequently, current response to voltage steps of different magnitude and direction was monitored. A wide range of potentials (+18 to −262 mV) was applied in decrements of 10 mV. The instantaneous current-voltage relation (*see arrow 1* in Fig. 6*a*) allows the study of the Ca^{2+} effect on the channel pore, whereas the influence of channel gating on the shape of the curve is eliminated. The finding that the strong voltage dependence of Ca^{2+} blockade, characteristic for the steady-state currents, is preserved in instantaneous current-voltage curves, may be interpreted as a rapid (≤5 msec) blockade of the open channel by Ca^{2+}. Instantaneous current amplitudes at potentials more positive than −60 mV were totally unaffected by external Ca^{2+}, indicating that a constant fraction of channels was activated by the prepulse (i.e., channel gating was unaffected by Ca^{2+}) and that Ca^{2+} was instantaneously expelled from the pore in this voltage range. Instantaneous current amplitudes were extrapolated by fitting current deactivation with a single exponential function. The first 5–10 msec were omitted from the fit to avoid contamination by capacitive current spikes. Extrapolation to infinity at potentials more positive than −100 mV, the "activation potential" of the inward rectifier, rendered the "leak" that was supposed to be linear over the whole voltage range. At potentials with incomplete deactivation of the inward rectifier (i.e., below −100 mV), the instantaneous current amplitude was calculated by adding the current amplitude of the tail and the residual current and subtracting the "leak." The residual current minus the "leak" yielded the steady-state current carried by the inward rectifier.

We tested if the Ca^{2+} effect could be interpreted in terms of an interaction of the blocking ion with a binding site within the electric field of the membrane (Woodhull, 1973). The ratio of blocked (R_b) and unblocked channels can be described as a function of the membrane potential (E) with the following Boltzmann equation (for details, *see* Discussion):

$$R_b/(1 - R_b) = a_{Ca^{2+}}/K_{0mV} * \exp(-\delta z FE/RT) \quad (2)$$

where: K_{0mV} = dissociation constant for Ca^{2+} at 0 mV, δ = electrical distance of the binding site, $a_{Ca^{2+}}$ = Ca^{2+} activity; z, F, R and T have their usual meaning. Plotting the ratio of blocked and unblocked current as a function of the membrane potential on a logarithmical scale leads to a linear relation (*see* Fig. 7), as should be expected if the model holds. Currents at 0.1 mM Ca^{2+} were considered to approximate those without Ca^{2+} and were therefore taken as a control (eliminating all Ca^{2+} would lead to a seal breakdown). From the slope of the lines fitted to the data, an electrical distance of about 0.2–0.5 at 10

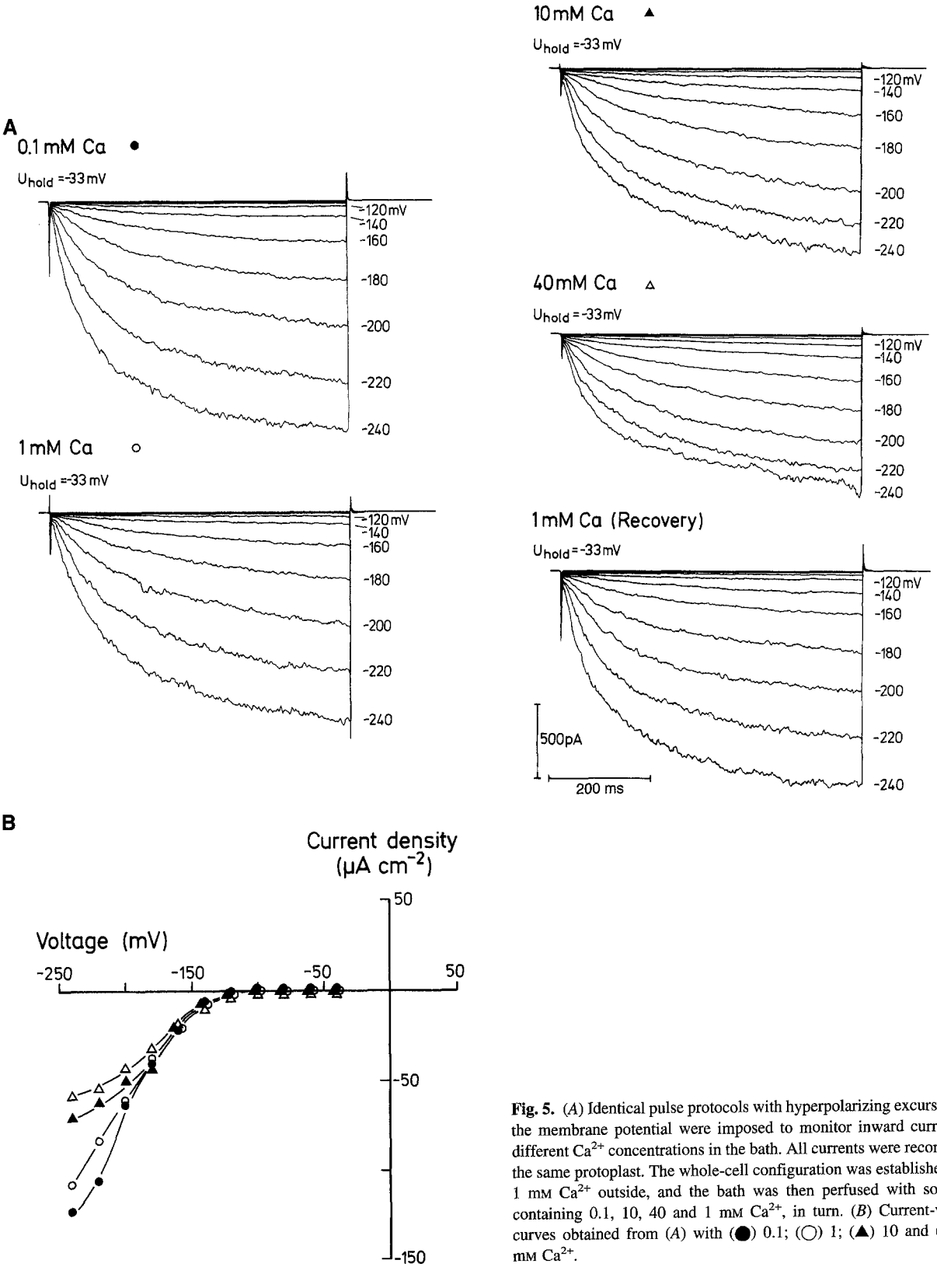

Fig. 5. (*A*) Identical pulse protocols with hyperpolarizing excursions of the membrane potential were imposed to monitor inward currents at different Ca^{2+} concentrations in the bath. All currents were recorded on the same protoplast. The whole-cell configuration was established with 1 mM Ca^{2+} outside, and the bath was then perfused with solutions containing 0.1, 10, 40 and 1 mM Ca^{2+}, in turn. (*B*) Current-voltage curves obtained from (*A*) with (●) 0.1; (○) 1; (▲) 10 and (△) 40 mM Ca^{2+}.

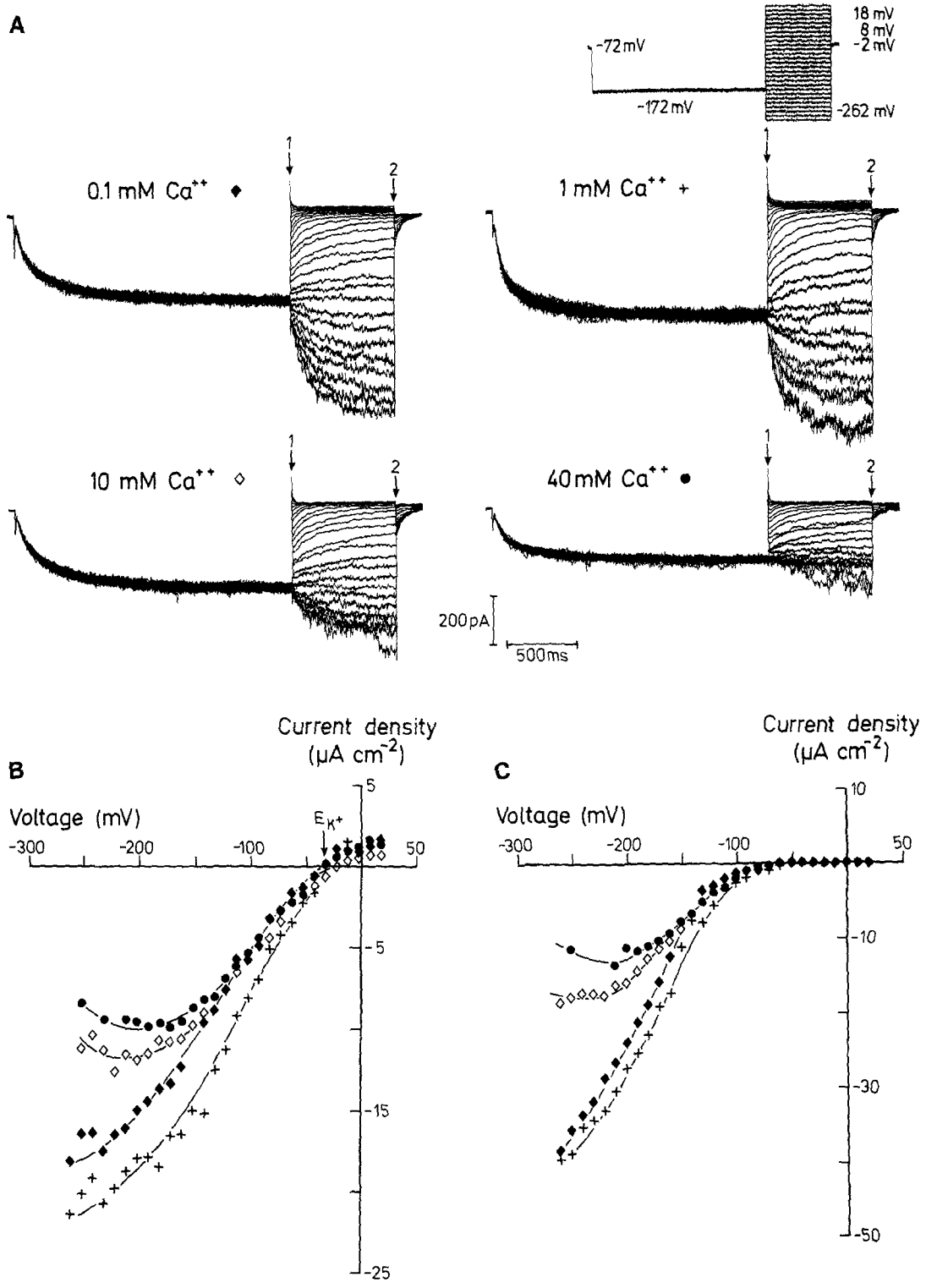

Fig. 6. (*A*) Performance of the inward rectifier in double-pulse experiments at different Ca^{2+} concentrations in the bath. The imposed pulse protocol is shown at the top, right. In the second pulse segment, the potential was varied for each sweep from 18 to −262 mV (10 mV decrements). Between each sweep, the membrane was kept at −72 mV for 10 sec. The two last sweeps at 40 mM Ca^{2+} were omitted, as the current signal became unsteady due to membrane breakdowns. (*B*) Instantaneous current-voltage curves for the experiment shown in *A* (*see arrow 1* at original traces) for (♦) 0.1 mM; +1 mM; (◇) 10 mM and (●) 40 mM Ca^{2+} in the bath. All curves intersected the voltage axis close to E_{K^+} (*see* arrow at reversal potential; 30 mM K^+ in the bath). Experiments were started with 1 mM Ca^{2+} (*see legend* Fig. 5). Currents with 1 mM Ca^{2+} are somewhat larger than those with 0.1 mM probably due to a slight, initial "rundown." (*C*) Steady-state current-voltage curves (*arrow 2* at current traces) after leak subtraction (♦) 0.1 mM; +1 mM; (◇) 10 mM; (●) 40 mM Ca^{2+}.

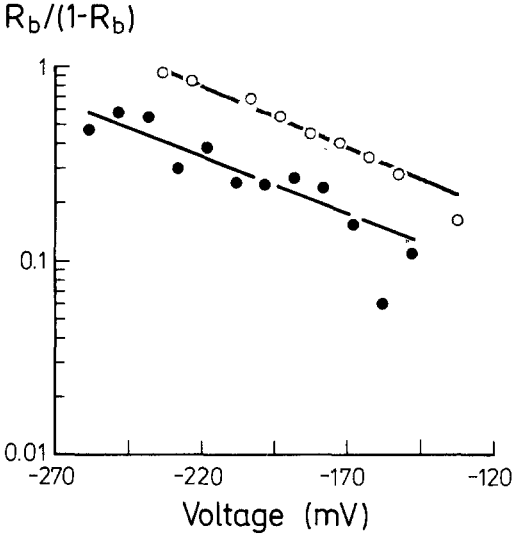

Fig. 7. Semilogarithmic plots of the ratio of blocked (R_b) to unblocked channels at 10 mM Ca^{2+} (●) and 40 mM Ca^{2+} (○) as a function of the membrane potential. The ratio was calculated from whole-cell currents at 0.1 and 10 or 40 mM Ca^{2+}, respectively, as follows: $R_b/(1 - R_b) = (I_{0.1Ca^{2+}} - I_{xCa^{2+}})/I_{xCa^{2+}}$. Data were taken from the experiment shown in Fig. 6. The linear relations were fitted with a Boltzmann function (Eq. 2; *see* continuous line). From the slope, the electrical distance for Ca^{2+} binding could be calculated (*see* Table 2). For this experiment, it was 0.17 and 0.19 at 10 and 40 mM Ca^{2+}, respectively.

and 40 mM Ca^{2+} could be calculated (*see* Table 2), the values varying somewhat between individual cells. Assuming the field strength along the pore to be constant, Ca^{2+} would have to penetrate about one-third of the transmembrane electric field to reach this binding site. Note that instantaneous current-voltage relations at different Ca^{2+} concentrations intersect the voltage axis at the same value, the reversal potential for K^+. No significant deviation of tail current reversal potentials from the Nernst potential for K^+ was observed at various gradients of Ca^{2+} (Table 3), indicating that currents are highly selective for K^+ over Ca^{2+} (*see also* Wegner & Raschke, 1994).

La^{3+}

Figure 8 shows current traces obtained with different La^{3+} concentrations and resulting current-voltage relations. The voltage dependence of inward currents was modified by La^{3+} in a characteristic way, including a shift of the "activation potential" (i.e., the potential below which time-dependent currents could be discerned) in the depolarizing direction and a slightly voltage-dependent reduction of the slope conductance. Quantitatively, the effect of La^{3+} on the K^+ chord conductance (Fig. 8*C*) could well be described by a shift of the open probabilities to more positive potentials (expressed as the shift of the voltage at which 50% of the channels are in the open state) and, simultaneously, an open channel blockage according to the Woodhull model, combining the Boltzmann terms in Eqs. 1 and 2 (*see* Appendix). The modification of channel gating could have been due to changes of the surface potential near the voltage sensor of the channel (Hille, Woodhull & Shapiro, 1975; McLaughlin & Harary 1976). From the combined fit, we obtained an electrical distance for the La^{3+} blockage of 0.10 ± 0.01 at 1 mM La^{3+} and 0.07 ± 0.02 at 10 mM La^{3+} (*see* Table 2). The validity of our approach could again be tested by applying double-pulse protocols (Fig. 9). Instantaneous current-voltage curves lacked the characteristic "La^{3+}-shift" observed with steady-state relations (*compare* Figs. 8*B* and 9*B*), indicating that this shift was exclusively due to an effect on channel gating. The reversal potential after addition of La^{3+} remained close to the Nernst potential of K^+, a good indication that La^{3+} had no effect on the selectivity of the inward rectifier and did not pass through the pore. Like Ca^{2+}, La^{3+} blocked instantaneous currents at hyperpolarization in a voltage-dependent manner. Applying the Woodhull model to these data, we calculated an electrical distance of 0.09 for the La^{3+} binding site (Fig. 10 and Table 2); that was remarkably close to the values calculated from steady-state conductances. It seems that La^{3+} action can thus be explained consistently by a masking of surface charges and, at the same time, a binding of the ion to a site within the electrical field of the plasma membrane.

Note, that La^{3+} was much more effective in blocking the inward rectifier than Ca^{2+} (*see* the dissociation constants at 0 mV, Table 2).

Modulation of channel kinetics by La^{3+} was consistent with this model of charge screening. The time course of current deactivation could well be described with a single exponential equation. The time constant was voltage dependent (*see* Fig. 11), increasing with hyperpolarization. In the presence of La^{3+}, the τ-U relation shifted to more positive potentials (Fig. 11) corresponding to the shift of the voltage dependence of gating. This means that the current deactivation is slowed down at a given voltage (*see inset*). Turning to the *activation* kinetics, a similar shift of the τ-U curve along the voltage axis was observed for the fast time constant in most experiments. This corresponds to a *decrease* of the time constant (i.e., the activation was faster with La^{3+}, *see* current traces in Fig. 5), resulting from the slope of the τ-U relation being positive.

Attempts to restore the current level before addition of the blocker by perfusing the bath with La^{3+}-free solution were only partly successful, probably due to residual La^{3+}.

Ba^{2+}

The effect of Ba^{2+} on inward K^+ currents is shown in Fig. 12. The experimental approach was similar to that for

Table 2. Parameters characterizing the blockade of the K^+ inward rectifier by Ca^{2+} and La^{3+}

	10 mM Ca^{2+}	40 mM Ca^{2+}	1 mM La^{3+}	10 mM La^{3+}	1 mM La^{3+}
δ	0.37 ± 0.17	0.32 ± 0.12	0.10 ± 0.01	0.07 ± 0.02	0.09 ± 0.01
K_{0mV} (mM)	>120	>120	2.63 ± 2.09	1.90 ± 1.23	2.05 ± 0.59
n	4	3	4	3	3

Characteristic parameters (δ = "electrical distance" of the binding site, K_{0mV} = dissociation constant of the ion at 0 mV) for the blockade of the inward rectifier by Ca^{2+} (*see* Fig. 6) and La^{3+} (*see* Figs. 8,9), calculated from instantaneous current-voltage curves (columns 1, 2 and 5) and, for La^{3+}, from conductance-voltage curves (column 3 and 4). Data were obtained from experiments like the ones shown in Figs. 6, 8 and 9 by applying the Woodhull-model (Eq. 2) of voltage-dependent blockade. (Figs. 7, 10).

Table 3. Reversal potentials of tail currents at different Ca^{2+} gradients across the plasma membrane

$[Ca]_i$/μM	$[Ca]_o$/mM	E_{rev}/mV	n	E_{K^+}/mV
1	0.1	−39; −36	2	−33.0
1	1	−31 ± 3	11	−33.0
1	10	−35 ± 5	8	−34.1
1	40	−32 ± 2	3	−35.8
1	100	−39	1	−37.2
10	40	−35, −40	2	−35.8

All "tail" currents were recorded at standard K^+ concentrations (pipette: 120 mM; bath: 30 mM). Slight variations in E_{K^+} result from differences in the ion strength due to varying Ca^{2+} levels in the bath. Deviations of reversal potentials of the inward rectifier from the Nernst potential of K^+ were not significant.

Ca^{2+} (as shown in Fig. 5). Barium ions blocked the inward rectifier in a voltage-independent way (Fig. 12*C*). To make sure that the interaction of Ba^{2+} with the channel protein had reached a steady-state (*compare* Armstrong, Swenson & Taylor, 1982) when the pulse protocol was imposed (usually about 2 min after the final concentration of Ba^{2+} in the bath was established), voltage ramp experiments (slope: 117 mV/sec) were performed before the pulse protocol was started and about 2 min after its completion. Current traces resulting from both ramps were almost identical (*not shown*).

In Fig. 12*D*, a dose-response curve for the Ba^{2+} effect on the K^+ inward rectifier is shown at −220 mV. Data were fitted with a K_i of 1.3 mM for Ba^{2+}-action (*see* continuous line).

Barium ions did not affect the kinetics of inward K^+ currents. The block of these currents by Ba^{2+} was, at least, partly reversible (*not shown*).

Discussion

Blockage of the K^+ Inward Rectifier by TEA^+, Ba^{2+} and La^{3+}

Inward currents in xylem parenchyma cells respond to TEA^+ and Ba^{2+}, two well-established blockers of K^+ channels in the animal kingdom (Hille, 1992). Tetraethylammonium seems to be quite an ineffective blocker on plant cells in general, in contrast to many animal cells (Ketchum & Poole, 1990) and has an especially low affinity for the inward rectifier (*see* Fig. 3 and Colombo & Cerana 1991; Blatt, 1992). KAT1, however, appears to be slightly more sensitive to TEA^+ (Schachtman et al., 1992). The low affinity as well as the voltage independence of the blockage in xylem parenchyma cells resemble the characteristics of TEA^+ action on the corresponding guard cell conductance (Blatt, 1992). Barium ions inhibit inward K^+ currents in xylem parenchyma cells with a K_i of about 1.3 mM (*see* Fig. 12*C*). This seems to be in the same order of magnitude as observed with guard cells (Schroeder et al., 1987) and the KAT1 expressed in oocytes (Schachtman et al., 1992).

Remarkably, the K^+ inward rectifier was also inhibited by La^{3+}. This demonstrates that La^{3+} is no specific blocker of Ca^{2+} channels in plant cells. Previously, Terry, Findlay and Tyerman (1992) had already shown that La^{3+} also partly blocks the outward rectifier in *Amaranthus* protoplasts. In *Chara,* La^{3+} is effective in suppressing action potentials irreversibly and, likewise, blocks K^+ and Cl^- channels (Tyerman, Findlay & Paterson, 1986; Smith, Walker & Smith, 1987; Beilby, 1990).

We did not study effects of organic K^+ channel blockers on the inward rectifier in xylem parenchyma cells. Recently, Obermeyer, Armstrong and Blatt (1994) have presented an elaborate study on the blockage of the inward rectifier in guard cells by α-dendrotoxin.

Multiple Effects of Di- and Trivalent Cations on the K^+ Inward Rectifier: Inferences with Respect to the Channel Structure

Each of the di- and trivalent cations tested in this study, Ca^{2+}, Ba^{2+} and La^{3+}, blocked inward K^+ currents, but modifications of current-voltage relationships were such that a different mode of action on the channel protein was inferred for each of these cations.

In the case of Ca^{2+} and La^{3+}, the blockage became more effective with a hyperpolarization of the membrane. Woodhull (1973) studied the inhibition of the

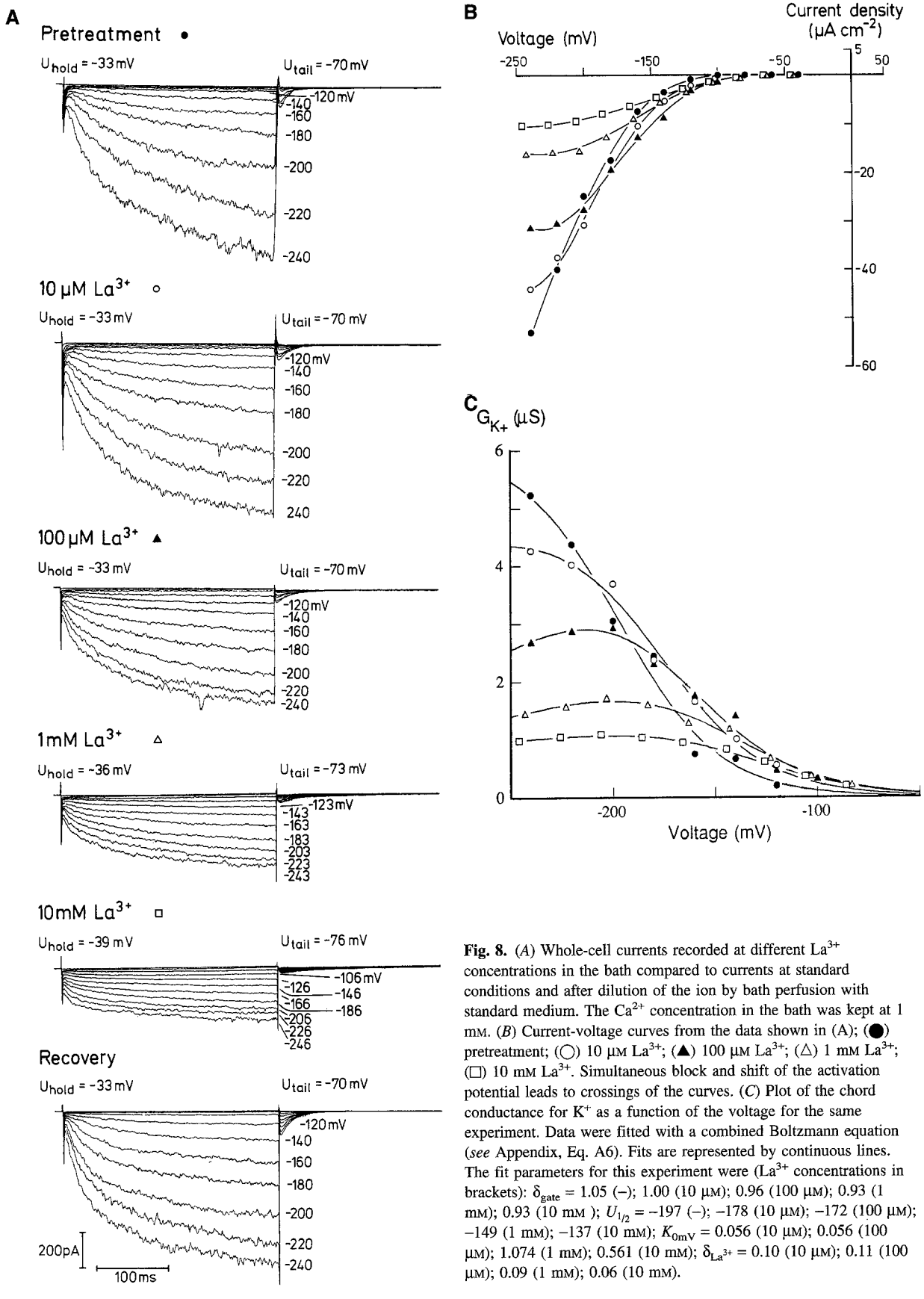

Fig. 8. (*A*) Whole-cell currents recorded at different La^{3+} concentrations in the bath compared to currents at standard conditions and after dilution of the ion by bath perfusion with standard medium. The Ca^{2+} concentration in the bath was kept at 1 mM. (*B*) Current-voltage curves from the data shown in (A); (●) pretreatment; (○) 10 µM La^{3+}; (▲) 100 µM La^{3+}; (△) 1 mM La^{3+}; (□) 10 mM La^{3+}. Simultaneous block and shift of the activation potential leads to crossings of the curves. (*C*) Plot of the chord conductance for K^+ as a function of the voltage for the same experiment. Data were fitted with a combined Boltzmann equation (*see* Appendix, Eq. A6). Fits are represented by continuous lines. The fit parameters for this experiment were (La^{3+} concentrations in brackets): δ_{gate} = 1.05 (–); 1.00 (10 µM); 0.96 (100 µM); 0.93 (1 mM); 0.93 (10 mM); $U_{1/2}$ = –197 (–); –178 (10 µM); –172 (100 µM); –149 (1 mM); –137 (10 mM); K_{0mV} = 0.056 (10 µM); 0.056 (100 µM); 1.074 (1 mM); 0.561 (10 mM); $\delta_{La^{3+}}$ = 0.10 (10 µM); 0.11 (100 µM); 0.09 (1 mM); 0.06 (10 mM).

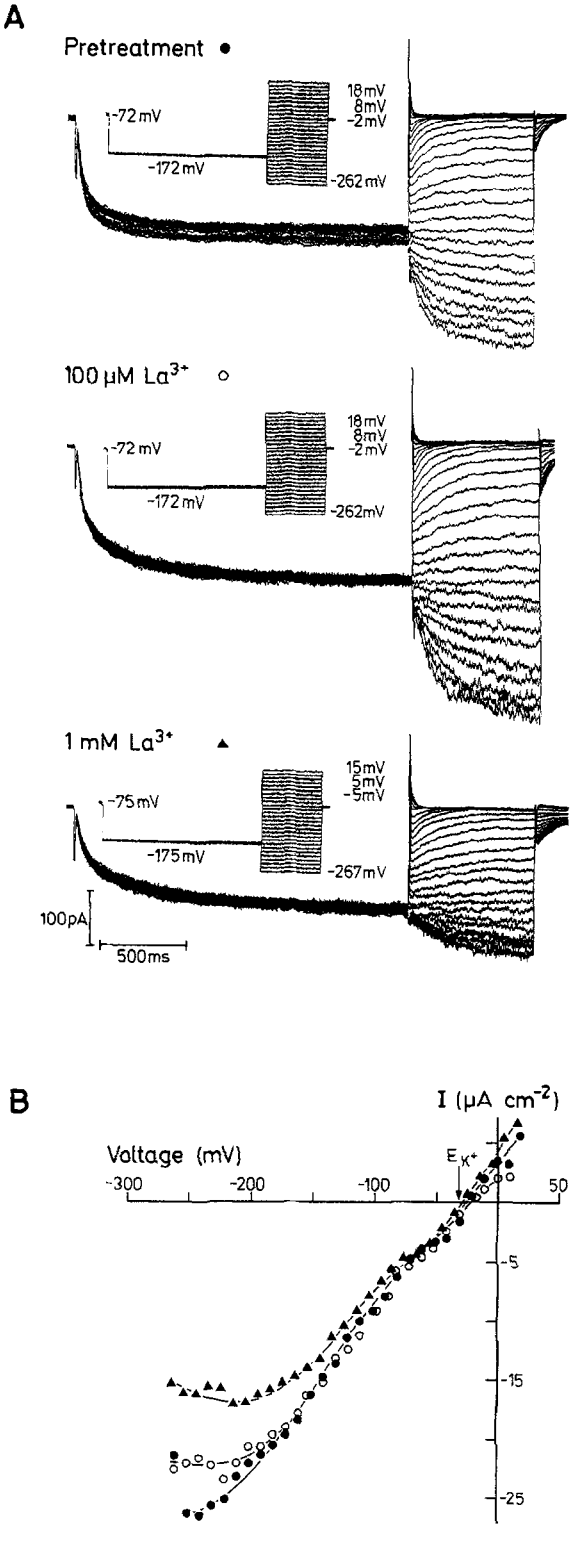

Fig. 9. (*A*) The effect of La^{3+} (100 µM and 1 mM) on the K^+ inward rectifier was tested over a wide voltage range by imposing double-pulse protocols (*see* Fig. 6). Pulse protocols are shown for each experiment. The Ca^{2+} concentration in the bath was 1 mM for this series of measurements. Instantaneous current-voltage relations (*B*) were extrapolated from activation and deactivation time courses (*see text*): (●) control; (○) 100 µM; (▲) 1 mM La^{3+}. Note that current-voltage curves passed through E_K.

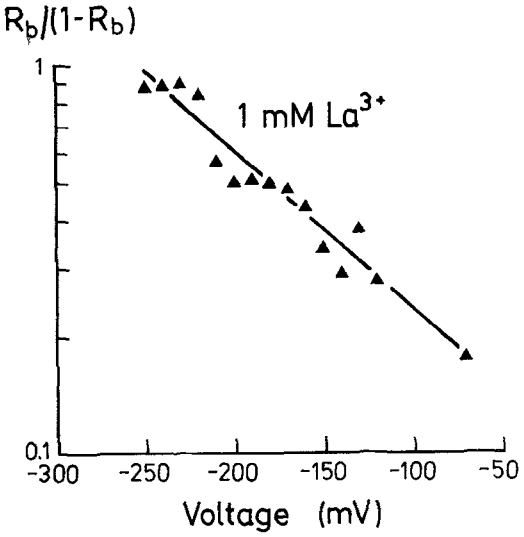

Fig. 10. Semilogarithmic plot of the fraction of blocked to unblocked channels *vs.* the clamped potential (*compare* Fig. 7) for 1 mM La^{3+} in the bath. Data were obtained from instantaneous current-voltage curves (Fig. 9). For this experiment, the electrical distance for La^{3+} binding was 0.09, the binding constant at 0 mV was 2.64 mM.

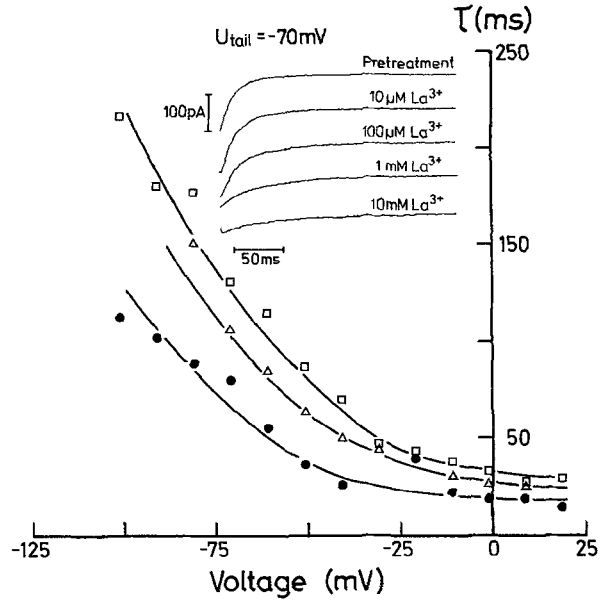

Fig. 11. Effect of La^{3+} on deactivation kinetics. The voltage dependence of the time constant is shown at pretreatment (●) and after addition of 0.1 (△) and 1 mM La^{3+} (□). Inset: tail current (−70 mV) at different La^{3+} concentrations in the bath. Note that voltages were not corrected for changes in surface charge in the presence of La^{3+}. Lines were drawn arbitrarily by eye.

Na^+ channel in frog nerve cells by protons and interpreted the voltage dependence of blockage in terms of an interaction of the inhibitor with a binding site located in the channel pore, within the electric field of the membrane. The Woodhull model was also applied to giant algal cells (Tester, 1988*b*) and to channels in the tono-

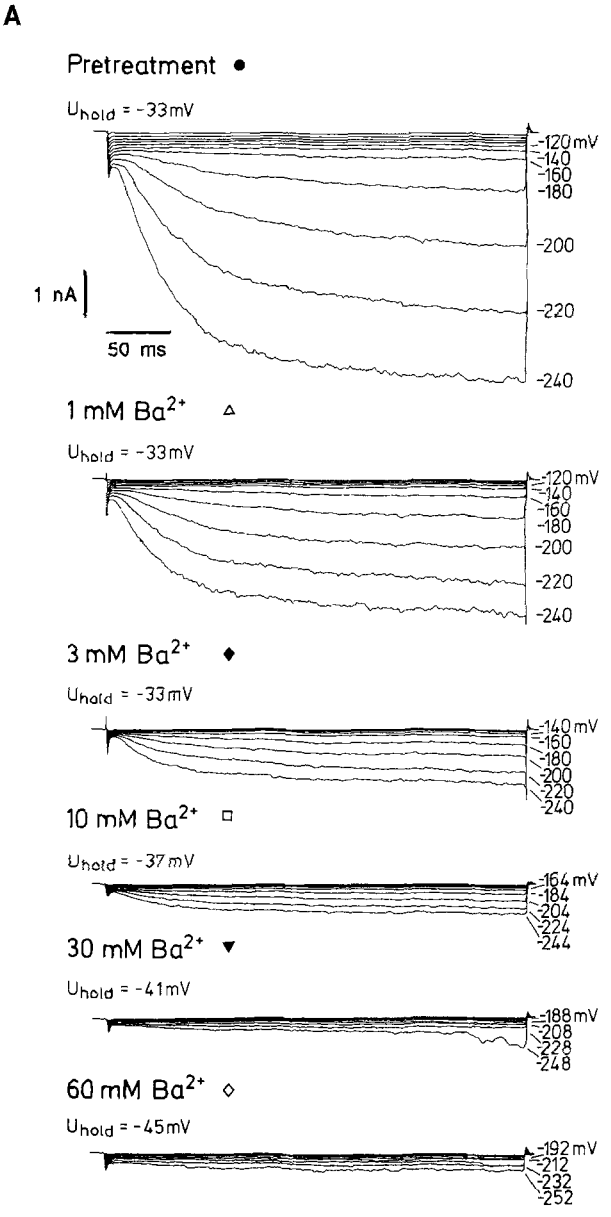

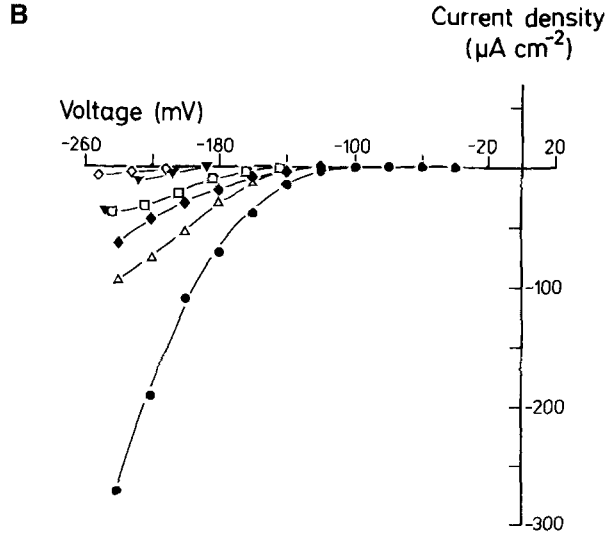

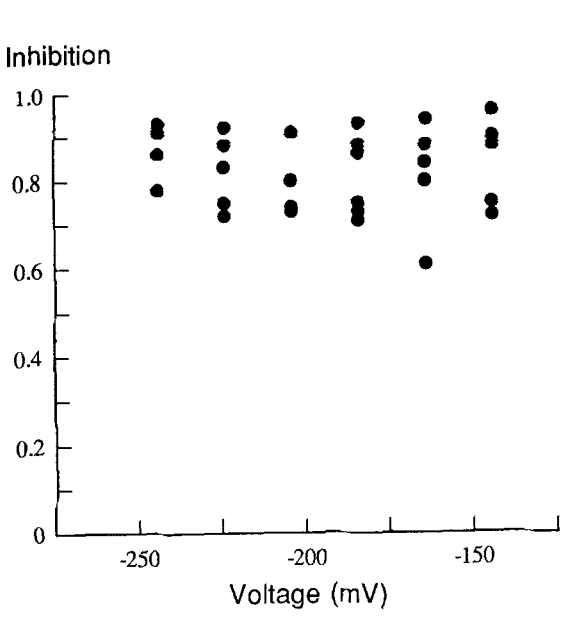

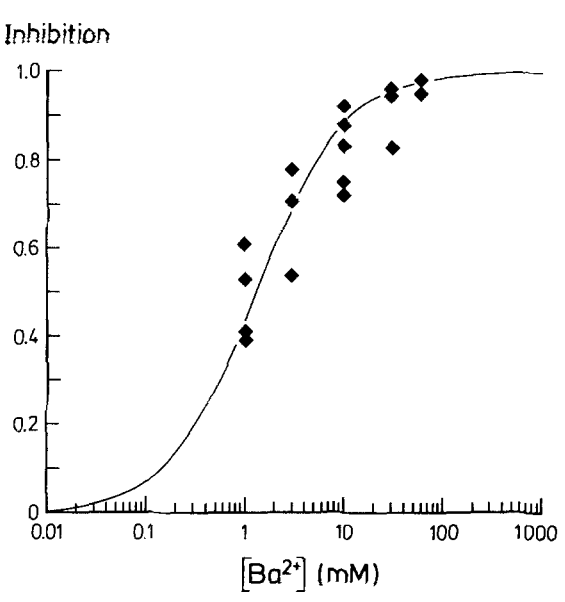

Fig. 12. (*A*) Effect of Ba^{2+} on the inward rectifier. Various concentrations of Ba^{2+} were applied to one protoplast clamped in the whole-cell configuration and superimposed current traces recorded at each concentration level are shown. Hyperpolarizing stimuli were applied in decrements of 20 mV (*see* potentials shown next to the traces). (*B*) Current-voltage curves (current densities) obtained from the experiment shown in *A*. (●) Pretreatment; (△) 1 mM Ba^{2+}; (♦) 3 mM Ba^{2+}; (□) 10 mM Ba^{2+}; (▼) 30 mM Ba^{2+}; (◇) 60 mM Ba^{2+}. (*C*) Plot of the fraction of channels clocked by Ba^{2+} (=inhibition) *vs.* the clamped potential. Data from six protoplasts with 10 mM Ba^{2+} in the bath are shown. (*D*) Dose-response curve (semilogarithmic) for Ba^{2+} action (five experiments). Fitting a continuous line to the data yielded a value of 1.3 mM for the K_i.

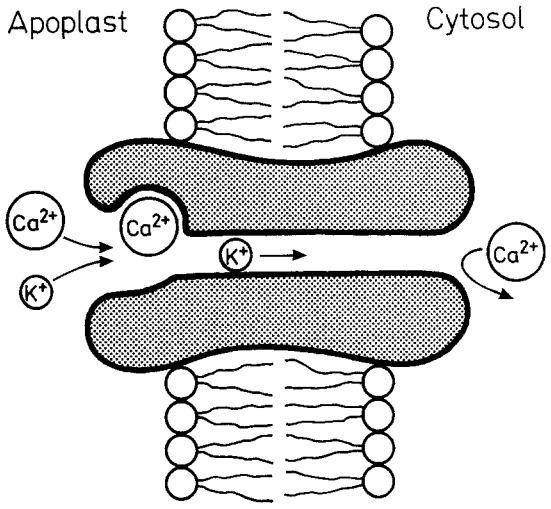

Fig. 13. This model of the K^+ inward rectifier summarizes our observations concerning Ca^{2+} action on the channel: Ca^{2+} invades the channel from the bath side and interacts weakly with a binding site in the pore. However, Ca^{2+} is not translocated and does not act on the channel from the inside (at least not in the range of concentrations tested here).

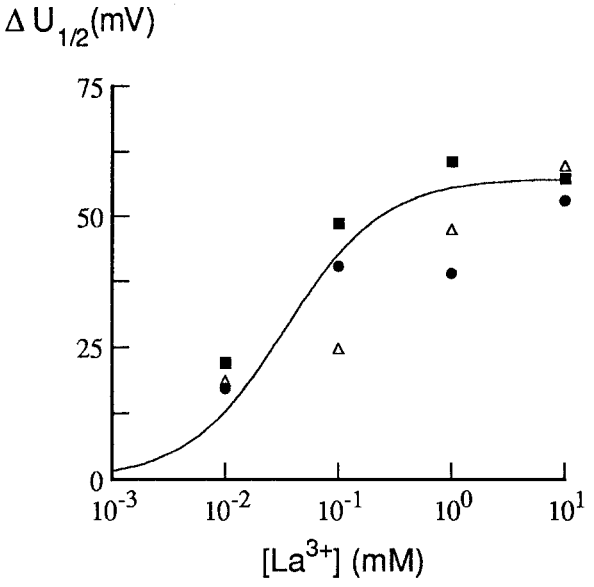

Fig. 14. Displacement of the voltage at which half of the channels are in the open state ($U_{1/2}$) for the inward rectifier after addition of La^{3+} to the bath as a function of the La^{3+} concentration (semilogarithmic plot). Data from three experiments are shown as indicated by different symbols. $U_{1/2}$ was obtained by fitting the voltage dependence of the chord conductance in the presence and absence of La^{3+} as described in the Appendix (*see* Fig. 8*C*). An apparent binding constant for La^{3+} to the membrane of 0.034 mM was estimated (*see* continuous line).

plast of higher plants (Weiser & Bentrup, 1993). Although the model seems to have its limitations (*see e.g.*, Eisenman & Horn, 1983; Draber, Schultze & Hansen 1992), it provides a means to derive information on the channel structure from electrophysiological measurements. Our view of the Ca^{2+} action on the K^+ inward rectifier, based on the application of the Woodhull model to our experimental data, is depicted in Fig. 13. Calcium ion enters the pore from the outside and interacts weakly with a binding site in the pore (Table 2). However, it seems not to pass the pore (Fig. 6), as the reversal potential with respect to K^+ was Nernstian (Table 3), and it does not enter the pore from the inside either as long as the concentration in the cytosol is kept at a physiological level (Fig. 4). In this model, the selectivity filter of the channel is located between the Ca^{2+} binding site and the cytosolic mouth of the channel; the value of 0.2–0.5 for the electrical distance of the Ca^{2+} blockage may be taken as an indication that the selectivity filter is positioned approximately halfway through the pore or beyond (with bath side as a reference).

Changes in the current-voltage characteristics were more complex when La^{3+} was added to the bath. They could be explained satisfactorily with a cooperation of two "independent" molecular effects: (i) a voltage-dependent blockade similar to that by Ca^{2+} (Fig. 9, *compare also* Fig. 6) and (ii) a shift in the voltage dependence of gating due to charge screening. The value for the electrical distance of La^{3+} blockage was 0.09, whereas the one for Ca^{2+} was about 0.2–0.5, indicating that both ions were acting on different binding sites. Lanthanum ion appeared to hardly enter the electrical field of the membrane; probably it binds to the mouth of the channel. Lanthanum ion is excluded from further penetration into the pore either as a consequence of electrostatic repulsion due to the high charge density of this ion or due to its high dehydration energy; for translocation through K^+ channels, ions need to be partly dehydrated (Yellen, 1987).

Further insight into the structure of the pore may be obtained from the permeability sequence of the channel and current-voltage relations in the presence of permeating ions other than K^+. Wegner and Raschke (1994) determined a selectivity sequence for the inward rectifier running $K^+ > Rb^+ \approx Cs^+ > Li^+ \approx Na^+$. This sequence was obtained from reversal potentials of tail currents under bi-ionic conditions. A comparison of instantaneous current-voltage relations, however, indicated that Rb^+ and Li^+ would change places in a sequence based on the conductance for these ions. This observation indicates that the channels involved acted as multi-ion file pores with several ions occupying the pore at different binding sites at a time. For Ca^{2+}, only one binding site was found; probably this is because Ca^{2+} has sole access to the outer part of the pore and, hence, is excluded from the occupation of additional sites that are located more closely to the inner face of the membrane.

Besides blocking the pore, La^{3+} caused a positive-going shift in the voltage dependence of gating (Fig. 14). A comparable effect, known as charge screening, is well established for action potentials in animal cells (Gilbert

& Ehrenstein, 1969; Hille et al., 1975) and has been described for the K^+ inward rectifier in guard cells (Blatt, 1992; Fairley-Grenot & Assmann 1992*b*) in the presence of elevated Ca^{2+} concentrations in the bath. According to the Guy-Chapman-Stern theory (McLaughlin, Szabo & Eisenman, 1971), adsorption or binding of cations to the outer membrane surface neutralizes negative charges that contribute to the transmembrane potential. The voltage shift for gating observed with La^{3+} occurred at concentrations as low as 10 μM (Figs. 8 and 14), whereas no such effect was seen with Ca^{2+} or Ba^{2+}, even if these ions were applied at concentrations about 1,000-fold higher. Charge screening in guard cells (Fairley-Grenot & Assmann, 1992*b*) and nerve cells (Hille et al., 1975) is less ion selective. The specificity of the effect in xylem parenchyma cells indicates that charge screening is exclusively due to binding of the ion, possibly to a domain of the channel protein that is involved in voltage sensing. Putative charge screening solely affected gating and had no effect on the reversal potential of the tail currents (Fig. 9).

The blockage of inward currents by Ba^{2+} was voltage independent; obviously, this ion does not penetrate into the channel pore. Binding seems to take place at a domain exposed to the outer membrane surface. The estimated binding constant of 1.3 mM is likely to be an underestimation, as the Ba^{2+} concentration close to the membrane surface is probably several times higher than the concentration in the bulk phase.

A Tentative Comparison of the K^+ Inward Rectifiers in Xylem Parenchyma Cells and in Guard Cells: Evidence for a Variation among K^+ Channels in Different Cell Types of Higher Plants

Here, we compare properties of the inward rectifier in guard cells, which has been studied extensively by several groups (Schroeder et al., 1987; Schroeder, 1988; Schroeder & Hagiwara, 1989; Blatt, 1992; Fairley-Grenot & Assmann, 1992*a,b*), and, as far as data are available, of KAT1 (Schachtman et al., 1992) with our findings on a similar inward rectifier in xylem parenchyma cells.

Gating properties of all three rectifiers appear to be analogous (Fig. 1 and Table 1). For the minimum gating charge and the potential at which 50% of the channels are in the open state, we obtained values for xylem parenchyma cells corresponding to those Blatt (1992) reported for guard cells. In both cell types, gating seems to be independent of the external K^+ concentration (*compare* Fig. 2 with data from Schroeder (1988) on guard cells). These observations seem to be in conflict with kinetic properties in whole-cell recordings: the inward rectifier in xylem parenchyma cells activated in a double-exponential manner (*see also* Findlay et al., 1994), whereas Fairley-Grenot and Assmann (1993) report on a single exponential time course in guard cells of *Vicia faba*. However, the time course for the inward rectifier is clearly multi-exponential in recordings on guard cells from the same species presented by others (*compare* current traces shown in Blatt (1992) (Fig. 1*A*); Schroeder et al., 1987). Activation kinetics was voltage dependent in intact guard cells (Blatt, 1992), but not in protoplasts (Fairley-Grenot & Assmann 1993). This variability, perhaps resulting from different experimental conditions, precludes a comparison of the kinetic properties of inward rectifiers in different systems at present.

Furthermore, rectifiers in guard cells and xylem parenchyma cells shared a sensitivity to TEA^+ and Ba^{2+} with KAT1 (Schachtman et al., 1992).

Clearly, the inward rectifiers differed in their Ca^{2+} dependence and selectivity. In guard cell protoplasts, K^+ inward currents were strongly reduced if the internal free Ca^{2+} concentration was raised from 100 nM to 1.5 μM (Schroeder & Hagiwara, 1989). No such effect was observed in xylem parenchyma protoplasts (*see* Fig. 4). Moreover, the inward rectifier in xylem parenchyma cells appears to be less permeable to Ca^{2+} than the one in guard cells (*compare* reversal potentials of tails in Table 3 with data reported by Fairley-Grenot and Assmann (1992*b*). A voltage-dependent blockage by externally applied Ca^{2+} seems to be common to both cell types (for guard cells, *see* Busch, Hedrich & Raschke, 1990; Fairley-Grenot & Assmann, 1992*b;* for xylem parenchyma cells, *see* Figs. 5, 6, 7 and Table 2). Although no detailed study is available for guard cells yet, the affinity for external Ca^{2+} appears to be considerably higher than in xylem parenchyma cells (*see* data shown by Busch et al., 1990). Both channels also differed in their permeability to Cs^+ (Wegner & Raschke, 1994). The selectivity of KAT1 was found to be similar to that of guard cells (Schachtman et al., 1992).

Conspicuously, properties related to channel gating seem to be common to all K^+ inward rectifiers, while channels differed in ion permeation, indicating a different topology of the pore. Genetic studies will bring to light whether the inward rectifiers form a gene family with tissue-specific expression, as preliminary results indicate (Schachtman et al., 1992), or if "fine-tuning" of properties occurs on a post-transcriptional level (Jan & Jan, 1990).

We admit that our studies on xylem parenchyma cells and those of others on guard cells were performed on different plant species. The possibility remains that variations are those between plant species rather than cell types. However, Fairley-Grenot and Assmann (1992*a,b;* 1993) compared K^+ currents in a dicot (*V. faba*) and a monocot (*Zea mays*) with respect to control by Ca^{2+} and found no differences between the K^+ inward rectifiers in both species.

Calcium and the Resorption of K^+ from the Xylem Sap

Variations in External Ca^{2+}

Though we could demonstrate an effect of the external Ca^{2+} concentration on the K^+ inward rectifier, the effective concentrations were well above those that have been reported to occur in the xylem sap, indicating that the blockage by Ca^{2+} is not of major physiological importance. Atkinson, Ruiz and Mansfield (1992) determined Ca^{2+} concentrations in the exudation sap of various monocots and dicots and obtained values ranging from 0.2 to 13.6 mM. Even at the maximum concentration measured, currents would only be reduced by 10 to 20% (*see* Figs. 5,6) and K^+ uptake into the xylem parenchyma would hardly be affected. The inward rectifier in guard cells is more sensitive to the external Ca^{2+} concentration, and circumstantial evidence has been obtained for a direct response of K^+ uptake to varying Ca^{2+} concentrations in the apoplast (Schwartz, 1985; Atkinson et al., 1992). The differences between K^+ uptake mechanisms in both cell types concerning external Ca^{2+} may be crucial in physiological terms.

Variations of Internal Ca^{2+}

In xylem parenchyma cells, potassium inward currents seem to remain unaffected by the cytoplasmic Ca^{2+} concentration within the physiological range. This observation is of major importance, as Ca^{2+} is known to act as a second messenger in guard cells and regulates the K^+ inward rectifier in these cells (Schroeder & Hagiwara, 1989). Signal transduction in xylem parenchyma cells may be organized in a different way, meeting their different function within the plant.

We would like to thank Drs. R. Kraayenhof, K. Krab and H. Miedema, Vrije Universiteit Amsterdam, for advice on surface potentials and Mr. Bernd Raufeisen, Göttingen, for his technical assistance during the preparation of the manuscript. Part of the experiments were performed with equipment provided to K.R. by the Deutsche Forschungsgemeinschaft. L.H.W. was supported by the Studienstiftung des Deutschen Volkes.

References

Anderson, J.A., Huprikar, S.S., Kochian, L.V., Lucas, W.J., Garber, R.F. 1992. Functional expression of a probable *Arabidopsis thaliana* potassium channel in *Saccaromyces cerevisiae. Proc. Natl. Acad. Sci. USA* **89:**3736–3740

Almers, W. 1978. Gating currents and charge movements in excitable membranes. *Rev. Physiol. Biochem. Pharmacol.* **82:**96–190

Armstrong, C.M., Swenson, R.P., Taylor, S.R. 1982. Block of squid axon K^+ channels by internally and externally applied barium ions. *J. Gen. Physiol.* **80:**663–682

Atkinson, C.J., Ruiz, L.P., Mansfield, T.A. 1992. Calcium in xylem sap and the regulation of its delivery to the shoot. *J. Exp. Bot.* **43:**1315–1324

Basset, M., Lepetit, M., Conejero, G., Sentenac, H. 1993. Structure and expression of the gene which encodes the AKT1 potassium channel of *Arabidopsis thaliana.* Abstract read at the symposium Membrane Transport in Plants and Fungi: Molecular Mechanisms and Control by the Society for Experimental Botany, Wye, UK

Beilby, M.J. 1990. Current-voltage curves for plant membrane studies: A critical analysis of the method. *J. Exp. Bot.* **41:**165–182

Blatt, M. 1992. K^+ channels of stomatal guard cells. Characteristics of the inward rectifier and its control by pH. *J. Gen. Physiol.* **99:**615–644

Blatt, M., Thiel, G., Trentham, D.R. 1990. Reversible inactivation of K^+ channels of *Vicia* stromatal guard cells following the photolysis of caged inositol 1,4,5-triphosphate. *Nature* **346:**766–769

Busch, H., Hedrich, R., Raschke, K. 1990. External calcium blocks inward rectifier potassium channels in guard cell protoplasts in a voltage- and concentration-dependent manner. *Plant Physiol.* **93(supplement):**96*A* (*Abstr.*)

Clarkson, D.T. 1993. Roots and the delivery of solutes to the xylem. *Philos. Trans. R. Soc. Lond. Ser. B* **341:**5–17

Colombo, R., Cerana, R. 1991. Inward rectifying K^+ channels in the plasma membrane of *Arabidopsis thaliana. Plant Physiol.* **97:**1130–1135

De Boer, A.H., Katou, K., Mizuno, A., Kjima, H., Okamoto, H. 1985. The role of electrogenic xylem pumps in K^+ absorption from the xylem of *Vigna unguiculata:* the effects of auxin and fusicoccin. *Plant, Cell Environ.* **8:**579–585

Draber, S., Schultze, R., Hansen, U.-P. 1991. Patch-clamp studies on the anomalous mole fraction effect of the K^+ channel in cytoplasmic droplets of *Nitella.* An attempt to distinguish between a multi-ion single-file pore and an enzyme kinetic model with lazy state. *J. Membrane Biol.* **123:**183–190

Eisenman, G., Horn, R. 1983. Ionic selectivity revisited: The role of kinetic and equilibrium processes in ion permeation through channels. *J. Membrane Biol.* **76:**197–225

Fairley-Grenot, K.A., Assmann, S.M. 1992*a*. Whole-cell K^+ current across the plasma membrane of guard cells from a grass: *Zea mays. Planta* **186:**282–293

Fairley-Grenot, K.A., Assmann, S.M. 1992*b*. Permeation of Ca^{2+} through K^+ channels in the plasma membrane of *Vicia faba* guard cells. *J. Membrane Biol.* **128:**103–113

Fairley-Grenot, K.A., Assmann, S.M. 1993. Comparison of K^+-channel activation and deactivation in guard cells from a dicotyledon (*Vicia faba*) and a graminaceous monocotyledon (*Zea mays*). *Planta* **189:**410–419

Findlay, G.P., Tyerman, S.D., Garrill, A., Skerrett, M. 1994. Pump and K^+ inward rectifiers in the plasmalemma of wheat root protoplasts. *J. Membrane Biol.* **139:**103–116

Führ, K.J., Warchol, W., Gratzl, M. 1993. Calculation and control of free divalent cations in solutions used for membrane studies. *Methods Enzymol.* **221:**149–157

Gilbert, D.L., Ehrenstein, G. 1969. Effect of divalent cations on potas-

sium conductance of squid axons: Determination of surface charge. *Biophys. J.* **9:**447–463

Hamill, O., Marty, A., Neher, E., Sakmann, B., Sigworth, F. J. 1981. Improved patch-clamp techniques for high-resolution current recordings from cells and cell-free membrane patches. *Pfuegers Arch.* **391:**85–100

Hedrich, R., Schroeder, J.I. 1989. The physiology of ion channels and electrogenic pumps in higher plants. *Annu. Rev. Plant Physiol.* **40:**539–569

Hille, B. 1992. Ionic Channels in Excitable Membranes. Second edition. Sunderland, MA

Hille, B., Woodhull, A.M., Shapiro, B.I. 1975. Negative surface charge near sodium channels in nerve: divalent ions, monovalent ions, and pH. *Philos. Trans. R. Soc. Lond. Ser. B* **270:**301–318

Jan, Y.L., Jan, Y.N. 1990. How might diversity of potassium channels be generated? *Trends Neurosci.* **13:**415–419

Ketchum, K.A., Poole, R.J. 1990. Pharmacology of the Ca^{2+}-dependent K^+ channel in corn protoplast. *FEBS Lett.* **274:**115–118

McLaughlin, S., Harary, H. 1976. The hydrophobic adsorbtion of charged molecules to bilayer membranes: A test of the applicability of the Stern equation. *Biochemistry* **15:**1941–1948

McLaughlin, S., Szabo, G., Eisenman, G. 1971. Divalent ions and the surface potential of charged phospholipid membranes. *J. Gen. Physiol.* **58:**667–687

Neher, E. 1992. Correction for liquid junction potentials in patch clamp experiments. *Methods Enzymol.* **207:**123–130

Obermeyer, G., Armstrong, F., Blatt, M.R. 1994. Selective block by α-dendrotoxin of the inward rectifier at the *Vicia* guard cell plasma membrane. *J. Membrane Biol.* **137:**249–259

Robinson, R.A., Stokes, R.M. 1968. The Debey-Hückel formula for the activity coefficient. *In:* Electrolyte Solutions, pp. 229–232. Butterworth, London

Schachtman, D.P., Schroeder, J.I., Lucas, W.J., Anderson, J.A., Garber, R.F. 1992. Expression of an inward-rectifying potassium channel by the *Arabidopsis* KAT1 cDNA. *Science* **258:**1654–1658

Schroeder, J.I. 1988. K^+ transport properties of K^+ channels in the plasma membrane of *Vicia faba* guard cells. *J. Gen. Physiol.* **92:**667–683

Schroeder, J.I., Hagiwara, S. 1989. Cytosolic calcium regulates ion channels in the plasma membrane of *Vicia faba* guard cells. *Nature* **338:**427–430

Schroeder, J.I., Raschke, K., Neher, E. 1987. Voltage dependence of K^+ channels in guard cell protoplasts. *Proc. Natl. Acad. Sci. USA* **84:**4108–4112

Schroeder, J.I., Thuleau, P. 1991. Ca^{2+} channels in higher plant cells. *The Plant Cell* **3:**555–559

Schwartz, A. 1985. Role of Ca^{2+} and EGTA on stomatal movements in *Commelina communis* L. *Plant Physiol.* **79:**1003–1005

Sentenac, H., Bonneaud, N., Minnet, M.M., Lacroute, F., Salman, J.-M., Garmard, F., Grignon, C. 1992. Cloning and expression in yeast of a plant potassium ion transport system. *Science* **256:**663–665

Smith, J.R., Walker, N.A., Smith, F.A. 1987. Potassium transport across the membranes of *Chara.* III. Effects of pH, inhibitors and illumination. *J. Exp. Bot.* **38:**778–787

Terry, B.R., Findlay, G.P., Tyerman, S.D. 1992. Direct effects of Ca^{2+} channel blockers on plasma membrane cation channels of *Amaranthus tricolor* protoplasts. *J. Exp. Bot.* **256:**1457–1473

Tester, M. 1988*a*. Blockade of potassium channels in the plasmalemma of *Chara corallina* by tetraethylammonium, Ba^{2+}, Na^+ and Cs^+. *J. Membrane Biol.* **105:**77–85

Tester, M. 1988*b*. Potassium channels in the plasmalemma of *Chara corallina* are multi-ion pores: Voltage-dependent blockade by Cs^+ and anomalous permeabilities. *J. Membrane Biol.* **105:**87–94

Tester, M. 1990. Tansley review No. 21. Plant ion channels: whole-cell and single-channel studies. *New Phytol.* **114:**305–340

Tyerman, S.D., Findlay, G.P., Paterson, G.J. 1986. Inward membrane current in *Chara inflata;* II. Effects of pH, Cl^- channel blockers and NH^{4+}, and significance for the hyperpolarized state. *J. Membrane Biol.* **89:**153–161

Wegner, L.H., Raschke, K. 1992. Ion channels in the plasmalemma of xylem parenchyma cells from roots of barley (*Hordeum vulgare* cv. Apex). *In:* Abstracts, 9th International Workshop on Plant Membrane Biology, Monterey. Vol. 53.

Wegner, L.H., Raschke, K. 1994. Ion channels in xylem parenchyma cells from barley roots: a procedure to isolate protoplasts from this tissue and a patch-clamp exploration of salt passageways into xylem vessels. *Plant Physiol.* **105:**799–813

Wegner, L.H., Raschke, K., De Boer, A.H. 1993. Properties of the inward rectifier in the plasmalemma of xylem parenchyma cells: evidence for a variation among K^+ channels in different cell types. *In:* Abstracts, Symposium of the Society of Experimental Botany on Membrane Transport in Plants and Fungi: Molecular Mechanisms and Control. Wye, Kent, UK

Weiser, T., Bentrup, F.W. 1993. Pharmacology of the SV channel in the vacuolar membrane of *Chenopodium rubrum* suspension cells. *J. Membrane Biol.* **136:**43–54

Woodhull, A.M. 1973. Ionic blockage of sodium channels in nerve. *J. Gen. Physiol.* **61:**687–708

Yellen, G. 1987. Permeation in potassium channels: Implications for channel structure. *Annu. Rev. Biophys. Biophys. Chem.* **16:**227–246

Appendix

The following formalism was developed to test the hypothesis that La^{3+} modulates inward K^+ currents by a combination of two "independent" molecular effects, namely a shift in the voltage sensitivity of the gate due to a screening of surface charges and a voltage-dependent blockage of the open channel within the electrical field of the membrane. It is assumed that charge screening only affects channel gating and has no bearing on ion permeation through the pore.

The K^+ chord conductance of the membrane resulting from currents passing through the inward rectifier can be described as follows:

$$G_{K+}(U) = n^* P_o(U)^* g_{\text{mean}}(U) \tag{A1}$$

with n being the total number of channels, $P_o(U)$ being the open probability and $g_{\text{mean}}(U)$ being the mean conductance of all channels in the open state.

The open probability of the inward rectifier can be described with the following Boltzmann term:

$$P_o(U) = 1/(1 + \exp[\delta_{\text{gate}} F\{U_{1/2} - U\}/RT]) \tag{A2}$$

(δ_{gate} = minimum equivalent gating charge, $U_{1/2}$ = voltage where 50% of the channels are in the open state; F, R and T have their usual meaning). The mean conductance of the open channels is a product of the unitary conductance g and the fraction of channels that is in the

unblocked state (i.e., without binding of La^{3+}). The unitary conductance is supposed to be ohmic:

$$g_{\text{mean}}(U) = g^*(1 - R_b(U)) \tag{A3}$$

with $R_b(U)$ being the fraction of channels blocked by La^{3+}. The relation of blocked to unblocked channels is expressed by the following relation according to the Woodhull model (Woodhull, 1973):

$$R_b/(1 - R_b) = a_{La^{3+}}/K_{0mV} * \exp(-\delta_{La^{3+}} zFU/RT) \tag{A4}$$

(K_{0mV} = dissociation constant for La^{3+} at 0 mV, $\delta_{La^{3+}}$ = electrical distance of the binding site for La^{3+}, $a_{La^{3+}} = La^{3+}$ activity; z, F, R and T have their usual meaning.) Inserting (A4) in (A3) and rearranging results in:

$$g_{\text{mean}} = \frac{g}{1 + a_{La^{3+}}/K_{0mV} * \exp(-\delta_{La^{3+}} zFU/RT)} \tag{A5}$$

Inserting (A5) and (A2) into (A1) renders an expression for the voltage dependence of the K^+ chord conductance:

$$G_{K^+}(U) = \frac{n * g}{(1 + \exp[\delta_{\text{gate}} F\{U_{1/2} - U\}/RT]) * (1 + a_{La^{3+}}/K_{0mV} * \exp[\delta_{La^{3+}} zFU/RT])} \tag{A6}$$